Journal of information and communication convergence engineering
http://jicce.org

J. Inf. Commun. Converg. Eng. 21(1): 1-8, Mar. 2023 Regular paper

An Accurate Design Method of Wideband BPF Considering Frequency Dependence of Inverters

Youna Jang[1]* and Dal Ahn[2], *Member*, *KIICE*

[1]Department of ICT Convergence, Soonchunhyang University, Asan, 31538, Republic of Korea
[2]Department of Electrical Engineering, Soonchunhyang University, Asan, 31538, Republic of Korea

Abstract

This paper presents a design method for a wideband bandpass filter (BPF) which compensates for frequency dependency based on the image admittance and image phase. In the proposed method, new compensation methods for the admittance and phase are integrated with the conventional method. The proposed method improves the frequency shift and reduces the unwanted bandwidth when designing more than 20% of the Fractional Bandwidth (FBW), whereas the conventional method exhibits frequency degradation at only 10% FBW. The proposed design theory was verified by applying it to both lumped elements and distributed lines through circuit simulation and measurements without an optimization process. The measurement results demonstrate improvements in the frequency shift and target bandwidth. In the future, an accurate design method based on frequency dependence can be implemented for the next-generation broadband communication system applications.

Index Terms: Frequency dependency, image admittance, image phase, inverter, Wideband BPF

I. INTRODUCTION

The use of impedance or admittance inverters in microwave bandpass filters (BPFs) is a practical and indispensable method to ensure that a microwave BPF has only one type of resonator, which simplifies its implementation. The equivalent circuit of a J or K-inverter is implemented using various approaches, such as through lumped or distributed lines, for practical applications. [1-3] implements a 90◦ transmission line by applying negative elements to an inverter, as shown in Figs. 1(a) and (b). These negative elements are absorbed into the resonators based on the resonator type. It can be difficult to remove the negative elements and obtain the desired in-band characteristics in the case of complex resonators. Additionally, these inverters have frequency-dependent parameters contrary to ideal inverters. This inverter dependence causes frequency degradation, resulting in a frequency narrower than that proposed by the filter design specifications.

Design optimization or iterative design techniques must be implemented to overcome the frequency degradation. Consequently, several frequency-compensating structures [4-8] have been proposed to achieve a wideband filter design, such as the use of various inverter types. [4] proposed a bandwidth contraction factor and center frequency deviation for a cavity filter to predict changes caused by frequency-dependent coupling structures. [5] proposed the use of ideal transformers with frequency-dependent turn ratios on both sides of the inverter and [6] proposed a generalized design technique to perform the practical compensation of discontinuity effects. The design methods proposed in [7-8] considered only the characteristic admittance variations of the inverter. Group delay compensation [9] and the use of coupled lines [10-12] have been proposed as wideband BPF design methods. Filters with open stubs have also been proposed by

Received 14 October 2022, **Revised** 20 December 2022, **Accepted** 6 January 2023
***Corresponding Author** Dal Ahn (E-mail: dahnkr@sch.ac.kr)
Department of Electrical Engineering, Soonchunhyang University, Asan 31538, Republic of Korea

Open Access https://doi.org/10.56977/jicce.2023.21.1.1 print ISSN: 2234-8255 online ISSN: 2234-8883

This is an Open Access article distributed under the terms of the Creative Commons Attribution Non-Commercial License (http://creativecommons.org/licenses/by-nc/3.0/) which permits unrestricted non-commercial use, distribution, and reproduction in any medium, provided the original work is properly cited.

Copyright ⓒ The Korea Institute of Information and Communication Engineering

based on the K-inverter structure [13]. However, the coupled lines have wideband limitation due to line spacing, and the methods proposed in [9-13] require optimization processes. Filter design methods using lumped elements [14-15] have been proposed to improve the design accuracy. Differences in the simulation and measurement are observed owing to the incomplete compensation of the frequency dependence of the lumped elements. Therefore, we employed the inverters depicted in Figs. 1(c) and (d) with no negative elements, which have not been analyzed for frequency-dependent compensation. The inverter structure for practical BPF implementation has a magnitude term as well as phase characteristics based on the frequency. A conventional circuit [16] was proposed to improve the frequency-dependent parameters based on a novel J-inverter model. However, only the phase compensation was performed in [16], and it still exhibited frequency degradation.

In this paper, we present an accurate design method for bandpass filters to compensate for the frequency dependence of the magnitude and phase terms. We compensate for the image admittance and phase terms that vary based on the frequency; consequently, the frequency degradation is improved from 10% to 20% Fractional Bandwidth (FBW). The proposed circuit is implemented using lumped elements and distributed lines, and the design theory is verified accordingly.

II. DESIGN THEORY OF BPF USING LUMPED CIRCUITS

A. ANALYSIS OF INVERTER TYPES AND CENTER FREQUENCY

It is difficult to design series resonators alternating with parallel resonators in the practical implementation of a BPF for high-frequency bands. In microwave filters, it is more practical to use J and K inverters [1], where a common design approach involves using a single type of resonator structure and impedance inverter. Fig. 1 depicts the four types of J-inverter models used for the implementation of BPFs since the resonator type is a shunt type. Figs. 1(a) and (b) depict the typical inverters with negative reactance values. The negative parameters are generally absorbed into the adjacent lines of the positive resonator. However, they are only applicable for cases where the proximity element values can absorb negative parameter values, which usually have a bandwidth limit. These inverters only exhibit the frequency dependency of the image admittance part, as shown in Table 1. Figs. 1(c) and (d) depict the modified inverter structures without any negative parameters. An idealized impedance or admittance inverter has characteristic immittances, K or J, and a phase shift of 90° at all frequencies. However, the practical inverter models for implementing the BPF structure exhibit a frequency dependency based on the image admittance and phase terms, as listed in Table 1. The conventional circuit [16] depicted in Figs. 1(c) and (d) has the frequency-dependent terms of image admittance corresponding to $\left(1-\frac{1}{\omega^2}\right) = 0$ or $(1-\omega^2 LC) = 0$, by applying $c = J/\omega_0$, $L = 1/\omega_0 J$. The image impedance (Z_{im}) in Fig. 1(c) is expressed as (1), indicating that Z_{im} is also a frequency-dependent function. Z_{im} in Fig. 1(d) is obtained in the same manner as in (1).

$$Z_{im} = \sqrt{\frac{AB}{CD}} = \sqrt{\frac{\frac{\omega_0}{jJ\omega}}{\left(2-\frac{1}{\omega^2 LC}\right)\frac{\omega_0 J}{j\omega}}} = \frac{1}{J}\frac{1}{\sqrt{2-\frac{1}{\omega^2 LC}}} \quad (1)$$

These frequency dependencies can cause frequency degradation of the designed filter with the widening of the frequency band owing to (1). Thus, the new J inverter values are obtained using (2-3) and the prototype values of the Chebyshev filter, g_n (n=0, …, 1), as follows:

$$J_{j,j+1}\sqrt{2-\left(\frac{\omega_0}{\omega}\right)^2} = \sqrt{\frac{B_{rj}B_{rj+1}}{g_j g_{j+1}}}\sqrt{2-\left(\frac{\omega_0}{\omega}\right)^2} \quad (2)$$

$$B'_{rj} = \frac{1}{\sqrt{2-\left(\frac{\omega_0}{\omega}\right)^2}}B_{rj} = \frac{\omega_0 C_{rj}}{\sqrt{2-\left(\frac{\omega_0}{\omega}\right)^2}}\left(\frac{\omega}{\omega_0}-\frac{\omega_0}{\omega}\right) \quad (3)$$

The center frequency, (ω_0), is obtained when the sum of susceptance at band edge frequencies, f1 and f2, are zero, as shown below:

$$B'_{rj}(\omega 1) + B'_{rj}(\omega 2) = 0$$

$$\omega_0 = \frac{\omega_1\omega_2}{\sqrt{\frac{\omega_1^2+\omega_2^2}{2}}} \quad (4)$$

The center frequency of the CLC type depicted in Fig. 1(d) can also be defined by applying the frequency variation term, $\sqrt{2-\omega^2 LC}$, in a similar manner as that of the LCL type, as follows:

$$\omega_0 = \sqrt{\frac{\omega_1^2+\omega_2^2}{2}} \quad (5)$$

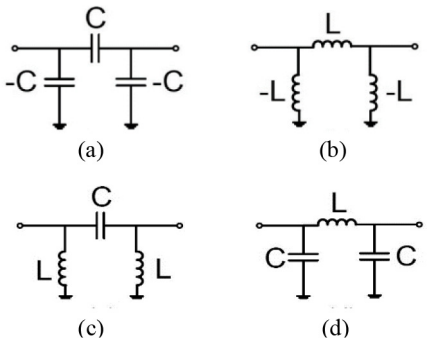

Fig. 1. Four types of J inverter models using lumped elements.

Table 1. Image admittance and phase of j inverter in Fig. 1

Type	Image admittance	Image phase
(a)	$J = \omega C$	$\beta = -90°$
(b)	$J = \omega L$	$\beta = +90°$
(c)	$j = \sqrt{\frac{C}{L}[2 - \frac{1}{\omega^2 LC}]}$	$\beta = +2sin^{-1}\sqrt{\frac{1}{2\omega^2 LC}}$
(d)	$j = \sqrt{\frac{C}{L}[2 - \omega^2 LC]}$	$\beta = -2sin^{-1}\sqrt{\frac{\omega^2 LC}{2}}$

B. PHASE COMPENSATION

The J inverter model, which employs a combination of lumped and distributed models that represent the inverter properties of certain discontinuities in the transmission lines [1], is also typically used for filter design. However, these types exhibit changes in their immittances as the frequency varies. This frequency dependency degrades the filter response since the inverter values do not vary linearly with the frequency [8]. These practical inverters require phase compensation for frequency variations to design a wideband bandpass filter. The image phase, $\phi = 2\sin^{-1}\sqrt{\frac{1}{2\omega^2 LC}}$, presented in Table 1(c) is the sum of the image phase at the center frequency (ϕ_0) and the phase deviations ($\Delta\phi$) from the image phase corresponding to the frequency.

$$1 - cos\phi = \frac{1}{\omega^2 LC} = \left(\frac{\omega_0}{\omega}\right)^2 = \left(\frac{\omega_0}{\omega_0 + \Delta\omega}\right)^2$$
$$= \left(1 - \frac{\Delta\omega}{\omega_0}\right)^2 = 1 - 2\frac{\Delta\omega}{\omega_0} \quad (6)$$

$$1 - cos\phi = 1 - \cos(\phi_0 + \Delta\phi) = 1 + sin\Delta\phi$$
$$= 1 + \Delta\phi \quad (7)$$

Thus, the phase deviations $\left(\frac{\Delta\phi}{2}\right)$ are expressed as $-\frac{\Delta\omega}{\omega 0}$ through (6-7) using trigonometric functions. The obtained phase deviations $\left(\frac{\Delta\phi}{2}\right)$ are applied to the modified J inverter shown in Fig. 2. Fig. 3 presents the proposed circuit diagram with a J-inverter for phase compensation.

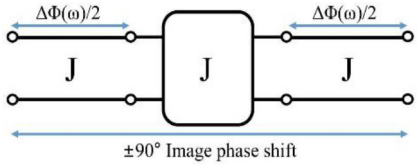

Fig. 2. The proposed inverter model for phase compensation.

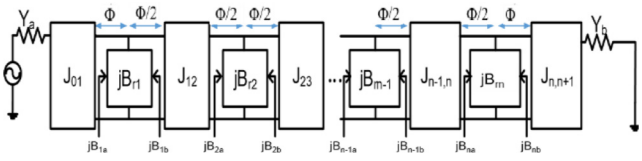

Fig. 3. The proposed circuit diagram with J inverter for phase compensation.

C. DESIGN OF BPF USING LUMPED ELEMENTS

The input admittance at each section of the J inverter was derived in [8] by using the correlation between the input impedance and load impedance to apply the amplitude and phase compensation terms. Thus, the derived input admittances can simplify the derivation of the formula for J_{01} in terms of Y_a, B_{1a}, and the prototype element values g_0 and g_1 as expressed as follows:

$$J_{01} = \alpha\frac{B'_{r1} + J_{12}\tan\frac{\Delta\Phi}{2} + J_{01}\tan\Delta\Phi}{J_{01} - \left(B'_{r1} + J_{12}\tan\frac{\Delta\Phi}{2}\right)\tan\Delta\Phi} \quad (8)$$

Through (8), J_{12} is derived as (9).

$$J_{12} = \frac{J_{01}^2 - (\alpha + B'_{r1})J_{01}\tan\Delta\Phi - B'_{r1}\alpha}{(\alpha + J_{01}\tan\Delta\Phi)\tan\frac{\Delta\Phi}{2}} \quad (9)$$

Similarly, except for the two stages of the input and output parts, $J_{i,i+1}$ is expressed as follows:

$$J_{i,i+1} = \left(J_{i-1,i}\cot(\delta_{i-1} + \Delta\Phi/2) - B'_{ri}\right)\cot\frac{\Delta\Phi}{2} \quad (10)$$
$$(i = 2,3,\ldots n-1)$$

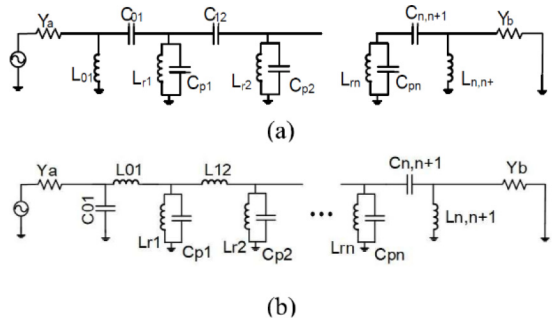

Fig. 4. (a) The n^{th} capacitive coupled BPF. (b) The n^{th} inductive coupled BPF.

Table 2. 3rd order calculated values using proposed design theory

	L01	C01	Lr1	Cr1	C12	Lr2
Conven	4.33	1.476	0.92	4.26	1.152	0.973
Proposed	4.44	1.467	0.92	4.35	1.217	0.961

(L[nH]/C[pF])

$J_{n,n+1}$ can be expressed as (11) and (12) using (10) and (8), respectively.

$$J_{n,n+1} = \left(J_{n-1,n}\cot(\delta_{n-1} + \Delta\Phi/2) - B'_{rn}\right)\cot\frac{\Delta\Phi}{2} \quad (11)$$

$$J_{n,n+1} = \frac{\zeta\tan\Delta\Phi}{2} \pm \sqrt{\frac{(\zeta\tan\Delta\Phi)^2}{4} + (\zeta - \beta)\beta}$$

where $$\alpha = \frac{Y_a}{\omega_1 g_0 g_1}, \beta = \frac{Y_b}{\omega_1 g_n g_n + 1}$$

$$\theta_{i-1} = \tan^{-1}\frac{B'_{ri-1} + J_{i-2,i-1}\tan\frac{\Delta\Phi}{2}}{J_{i-1,i}}$$

$$\delta_{i-1} = \tan^{-1}\left(\frac{1}{g_i - 1 g_i}\tan\left(\theta_{i-1} + \frac{\Delta\Phi}{2}\right)\right)$$

$$\zeta = B'_{rn} + J_{n-1,n}\tan\frac{\Delta}{2} + \beta \quad (12)$$

Therefore, the final equations, (11) and (12), must be identical according to the inverter formula. J_{01} was obtained using the recursive formula method, and the J inverter values of the other stages are obtained in order. The proposed circuit can be designed using an LCL-type of J inverter by applying the method of compensating for the magnitude and phase, as shown in Fig. 4. Table 2 presents the element values of the 3rd capacitive coupled BPF, which is calculated using the proposed design method.

III. SIMULATION AND FABRICATION RESULTS OF THE LUMPED ELEMENTS

The capacitively coupled BPFs with an FBW of 20% of the proposed circuit and a conventional circuit using inverter structures were designed at a center frequency of 2 GHz. Fig. 5 (top) and (bottom) depicts the mathematical comparison results of the circuit simulation corresponding to the conventional and proposed circuits, for the 3rd and 5th orders, respectively.

The frequency band of the 3rd conventional circuit shifts by approximately 20 MHz owing to the frequency variation term. The bandwidth of the conventional method was obtained only at approximately 340 MHz. However, the proposed circuit had a bandwidth of 380 MHz at a return loss of 16.4 dB. The 5th order BPF of the proposed circuit is also compensated for approximately 20 MHz frequency degradation, as shown in Fig. 5(bottom). Fig. 6 depicts the 5th inductive coupled BPF using the CLC type, which demonstrates that the frequency shift is compensated by using a method similar to that of the capacitive-coupled BPF. Figs. 7(a) and (b) present the photographs of the conventional and proposed circuits, respectively. The fabricated substrate was Taconic, with a dielectric constant of 2.97, tangent delta of 0.001, copper thickness of 0.035 mm, and substrate height of 0.762 mm. The inductor elements of the 3rd capacitive coupled BPF were implemented by using a short stub, and the capacitor elements used chip capacitors. The chip capacitor values of the conventional circuit were 1.485 pF and 1.421

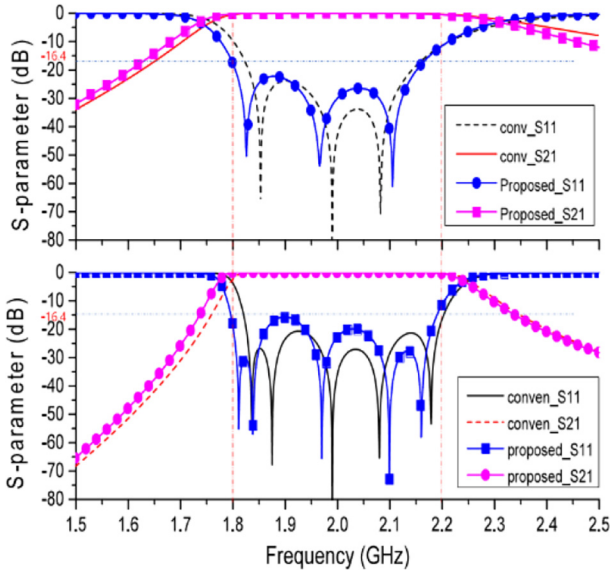

Fig. 5. Circuit comparison results from mathematical analysis of conventional and proposed circuits (Top) 3rd BPF (bottom) 5th BPF.

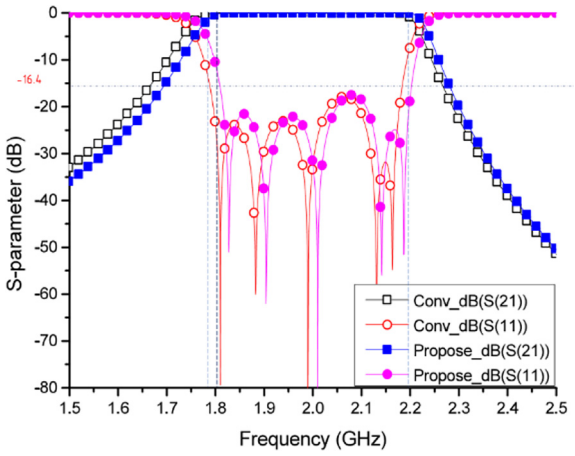

Fig. 6. The 5th inductive coupled BPF of the proposed circuit.

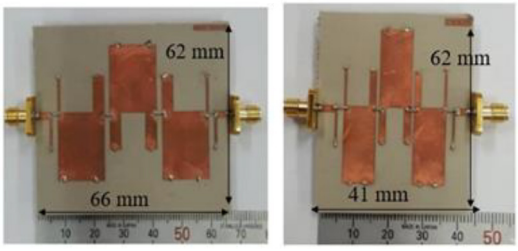

Fig. 7. Fabricated photograph of the (a) conventional filter and (b) proposed filter.

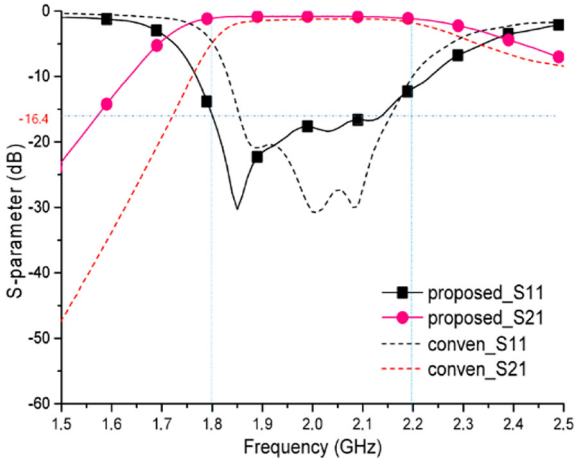

Fig. 8. Measured results of the conventional and proposed circuit of 3rd BPF.

pF, whereas those of the proposed circuit were 1.485 pF and 1.5 pF. The dimensions of the conventional and proposed circuits were 66×62 mm^2 and 41×62 mm^2, respectively. Fig. 8 presents the measurement results of the proposed circuit, which demonstrate that the frequency band of the conventional circuit is shifted by approximately 20 MHz owing to frequency degradation, whereas the proposed circuit fits the target bandwidth well.

IV. A DESIGN OF THE PROPOSED FILTER USING DISTRIBUTED LINES

The conversion from the LCL inverter to the distributed line demonstrates that the phase is slightly shifted from lumped elements to distributed lines, as shown in Fig. 9.

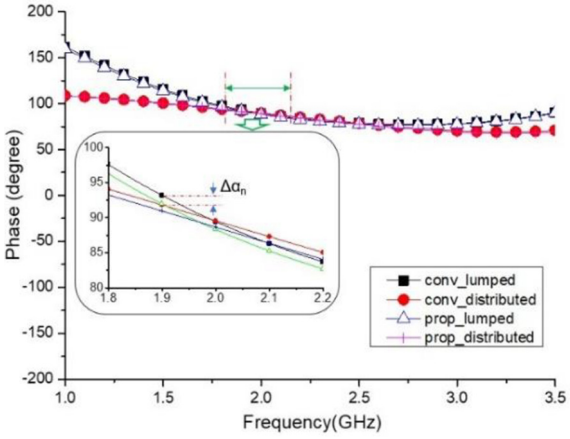

Fig. 9. Phase comparison results of conventional and proposed inverter circuit based on the lumped and distributed line.

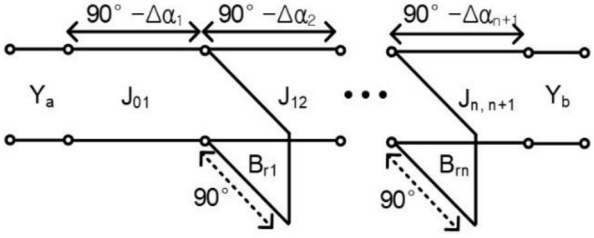

(a)

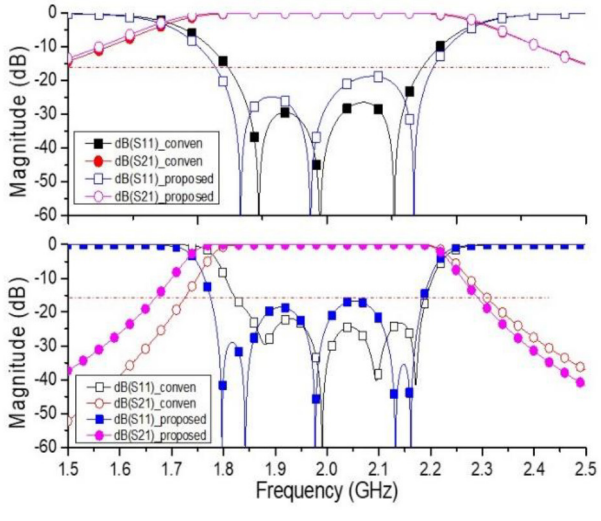

(b)

Fig. 10. (a) The proposed circuit comprising distributed lines. (b) Simulation results of the proposed 3rd and 5th filters in Fig. 10(a).

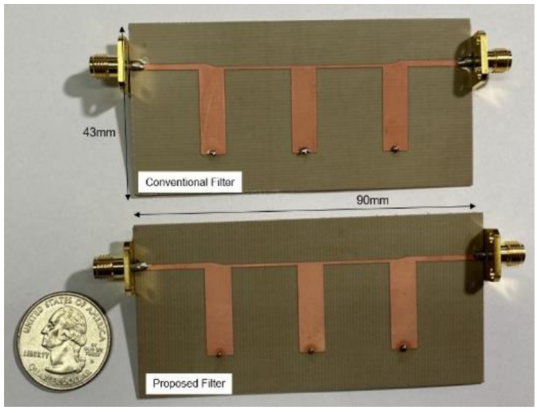

Fig. 11. Fabricated photograph of the proposed circuit using distributed lines.

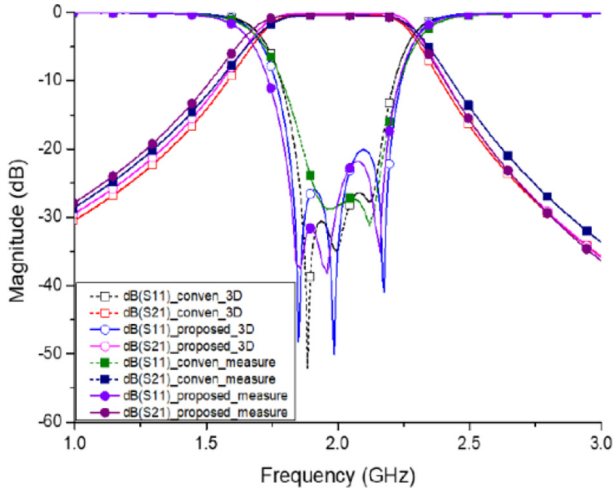

Fig. 12. Comparison results of the conventional and proposed filter based on 3D simulation and measurement.

Table 3. Performance comparison of previous works

Ref	f_0[MHz]	FBW[%]	RL[dB]	IL[dB]	Technology
[8]	2600	2.5	28	-	Waveguide
[11]	1990	12.4	18	1.4	Coupled line
[12]	2400	18.5	9.13	2.74	Coupled line
[13]	1450	42.7	13	-	LC-chips
This	2000	19	16.4	0.85	Transmission-line

Fig. 10(a) presents a circuit schematic of the application of distributed lines, and Fig. 10(b) presents the results of compensating for the phase error while converting from lumped elements to distributed lines in the circuit. The target FBW of 20% was well matched by compensating for the frequency-dependent terms, as a simulation result of the 3rd proposed filter. The conventional filter has a bandwidth of only 370 MHz, which does not reach the target band owing to its frequency degradation characteristics.

V. FABRICATION RESULTS OF BPF USING DISTRIBUTED LINES

Fig. 11 presents the photographs of the conventional and proposed filters. The proposed filter is implemented on a microstrip on a taconic substrate. The size of the fabricated filter was approximately 90×43 mm^2, at a center frequency of 2 GHz. Only the frequency shift due to the added junctions between the lines was slightly corrected when designing the 3D structure. The corrected values owing to the junctions were applied equally to the conventional and proposed circuits, which were fabricated without further optimization. Fig. 12 presents the comparison results of the conventional and proposed filters based on 3D simulations and measurements. Based on this fabrication process, the conventional filter can be used to design a BPF with 10% FBW. However, it does not accurately compensate for the frequency-dependent terms of magnitude and phase; therefore, it exhibits frequency degradation, as shown in Fig. 12. The conventional circuit exhibits a frequency degradation of 1.84-2.19 GHz at a return loss of 16.4 dB, and presents a narrower band and frequency shift. However, the proposed circuit exhibits a frequency degradation of 1.78-2.199 GHz at a return loss of 16.4 dB and has 20% FBW of the desired band.

Contrary to the LCL structure, which has a slightly smaller bandwidth owing to the high-pass filter type, the proposed circuit is well implemented, with phase compensation implemented by a distributed line, even with a target bandwidth of 20%.

Table 3 presents the comparison results of previous studies, which demonstrate the performance of the bandpass filter using the J/K inverter method.

VI. CONCLUSION

In this study, we present a wideband BPF design method using a lumped-type J inverter. The frequency-dependent function in the inverter of the lumped type is compensated for based on the magnitude and phase terms, to make a wideband filter. For magnitude compensation, the amplitude parameters changed by frequency were included in the susceptance to obtain a new J-inverter parameter. For the phase compensation, the J-recursive formula was used by applying the conventional J-inverter model. Thus, frequency degradation at 20% FBW was observed owing to the limitation of the amplitude-frequency compensation in the conventional structure. Therefore, the proposed circuit using lumped elements accurately compensated for the frequency shift and bandwidth, and it was confirmed that compensation was achieved even when implemented as a distributed line.

ACKNOWLEDGMENTS

This research was supported by the MSIT (Ministry of Science and ICT), Korea, under the ICAN (ICT Challenge and Advanced Network of HRD) program (IITP-2023-2020-0-01832) supervised by the IITP (Institute of Information & Communications Technology Planning & Evaluation), "Regional Innovation Strategy (RIS)" through the National Research Foundation of Korea (NRF) funded by the Ministry of Education (MOE) (2021RIS-004) and the Soonchunhyang University Research Fund.

REFERENCES

[1] G. Matthaei, L. Young, and E. M. Jones, "Microwave filters, impedance-matching networks and coupling structures," *Artech House Inc.*, pp. 775-809, Norwood, MA 1980.

[2] S. B. Cohn, "Direct-coupled-resonator filters," *Proceedings of the IRE*, vol. 45, no. 2, pp. 187-196, Feb. 1957. DOI: 10.1109/JRPROC.1957.278389.

[3] D. Budimir, "Generalized filter design by computer optimization," Artech House Inc., Mar. 1998.

[4] L. Young, "Direct-coupled cavity filters for wide and narrow bandwidths," *IEEE Transactions on Microwave Theory and Techniques*, vol. 11, no. 3, pp. 162-178, May 1963. DOI: 10.1109/TMTT.1963.1125629.

[5] R. Levy, "Theory of direct-coupled-cavity filters," *IEEE Transactions on Microwave Theory and Techniques*, vol. 15, no. 6, pp. 340-348, Jun. 1967. DOI: 10.1109/TMTT.1967.1126471.

[6] R. Levy, "A generalized design technique for practical distributed reciprocal ladder networks," *IEEE Transactions on Microwave Theory and Techniques*, vol. 21, no. 8, pp. 519-526, Aug. 1973. DOI: 10.1109/TMTT.1973.1128051.

[7] J. B. Lim, C. W. Lee, and T. Itoh, "An accurate CAD algorithm for E-plane type bandpass filters using a new passband correction method combined with the synthesis procedures," in *IEEE International Digest on Microwave Symposium*, Dallas, USA, vol. 3, pp. 1179-1182, 1990. DOI: 10.1109/MWSYM.1990.99789.

[8] H. Y. Hwang and S-W Yun, "The design of bandpass filters considering frequency dependence of inverters," *Microwave Journal (Euro-global edition)*, vol. 45, no. 9, pp. 154-163, Sep. 2002.

[9] T. Shao, Z. Wang, S. Fang, H. Liu, and Z. N. Chen, "A group-delay-compensation admittance inverter for full-passband self-equalization of linear-phase band-pass filter," *AEU-International Journal of Electronics and Communications*, vol. 123, Aug. 2020. DOI: 10.1016/j.aeue.2020.153297.

[10] J-R. Lee, J-H. Cho, and S-W Yun, "New compact bandpass filter using microstrip λ/4 resonators with open stub inverter," *IEEE Microwave and Guided Wave Letters*, vol. 10, no. 12, pp. 526-527, Dec. 2000. DOI: 10.1109/75.895091.

[11] Y-S. Lin, C-H. Wang, C-H. Wu, and C. H. Chen, "Novel compact parallel-coupled microstrip bandpass filters with lumped-element K-inverters," *IEEE Transactions on Microwave Theory and Techniques*, vol. 53, no. 7, pp. 2324-2328, Jul. 2005. DOI: 10.1109/TMTT.2005.850445.

[12] S. Zhang and L. Zhu, "Synthesis method for even-order symmetrical chebyshev bandpass filters with alternative J/K Inverters and /spl lambda//4 resonators," *IEEE Transactions on Microwave Theory and Techniques*, vol. 61, no. 2, pp. 808-816, Feb. 2013. DOI: 10.1109/TMTT.2012.2233748.

[13] N. Intarawiset, S. Akatimagool, and S. Narongkul, "Analysis of microwave filter based on LC chips in microstrip circuitry using K-inverter approach," in *6th International Conference on Technical Education (ICTechEd6)*, Bangkok, Thailand, pp. 1-4, 2019. DOI: 10.1109/ICTechEd6.2019.8790917.

[14] T. Matsumura, S. Ono, and K. Wada, "Compact dualband BPF composed of LC J-inverters using lumped elements," *Transactions of The Japan Institute of Electronics Packaging*, vol. 14, pp. E20-014-1-E20-014-10, Jul. 2021. DOI: 10.5104/jiepeng.14.E20-014-1.

[15] D. Ahn, S. H. Myoung, H.T. Kang, Y. W. Lee, C. S. Kim, J. S. Park, and J. B. Lim, "Accurate recursive inverter formula for the correction of phase variation effect on bandpass filters," in *1999 29th European Microwave Conference*, Munich, Germany, pp. 203-206, 1999. DOI: 10.1109/EUMA.1999.338508.

[16] Y. N. Jang, J. S. Kim, J. S. Ha, D. S. Kim, J. S. Lim, S. M. Han, and D. Ahn, "A design method of wideband BPF considering frequency dependence of inverters for SAW filter," in *IEEE MTT-S International Microwave Filter Workshop (IMFW)*, Perugia, Italy, pp. 185-188, 2021. DOI: 10.1109/IMFW49589.2021.9642283.

Youna Jang

received her master's degree in Display Engineering from Hanyang University, Seoul, Korea, in 2014. She also received her Ph.D. in Electrical Communication System Engineering from Soonchunhyang University, Choongnam, Korea, in 2019. She participated as a designer of the Duplexer filter in an internship program in 2015 at Qorvo, Bundang, South Korea. She was a lecturer at Soonchunhyang University from 2016 to 2020. She is currently a research professor at the Radio and Mechatronics Research Center. Her research areas include the design of passive components in microwave bands.

Dal Ahn

received his B.S., M.S., and Ph.D. degrees in Electronics from Sogang University, Seoul, Korea, in 1984, 1986, and 1990, respectively. From 1990 to 1992, he worked with the Mobile Communications Division, Electronics, and Telecommunications Research Institute (ETRI), Daejeon, Korea. Since 1992, he has been affiliated with the School of Electrical and Electronic Engineering, Soonchunhyang University, Asan, Chungnam, Korea, where he is currently a professor. Currently, he is also the chief of the RF and Microwave Component Research Center (RAMREC), Soonchunhyang University. He is also a technical consultant for Tel Wave Inc., Suwon, Korea. Prof. Ahn is also an editor of the Journal of Korea Electromagnetic Engineering Society and a senior member of the Korea Electromagnetic Engineering Society (KEES). His current research interests include the design and application of passive and active components at radio and microwave frequencies, the design of RF front-end modules for various handset systems using low-temperature co-fired ceramic (LTCC) technology, DGS circuit applications, and circuit modeling using a commercial EM analysis program.